Biosensors and Bioelectronics 178 (2021) 113016

Contents lists available at ScienceDirect

Biosensors and Bioelectronics

journal homepage: http://www.elsevier.com/locate/bios

Low fouling electrochemical biosensors based on designed Y-shaped peptides with antifouling and recognizing branches for the detection of IgG in human serum

Min Chen, Zhen Song, Rui Han, Yang Li, Xiliang Luo *

Key Laboratory of Optic-electric Sensing and Analytical Chemistry for Life Science, MOE, Shandong Key Laboratory of Biochemical Analysis, College of Chemistry and Molecular Engineering, Qingdao University of Science and Technology, Qingdao, 266042, PR China

ARTICLE INFO

Keywords:
Electrochemical biosensor
Antifouling
Y-shaped peptide
Human IgG
Serum

ABSTRACT

The nonspecific adsorption and accumulation of biomolecules on electrode interfaces remains a challenge for sensitive and accurate detection of disease markers in complex biological media, and it is highly desired to develop antifouling biosensors capable of assaying targets in complicated real liquids. Herein, an efficient and simple antifouling biosensor was constructed based on a self-designed Y-shaped peptide. The Y-shaped peptide was designed with two branches: one branch with the peptide sequence of EKEKEKE for antifouling, and the other branch with the peptide sequence of HWRGWVA for recognizing of human IgG. Under optimized experimental conditions, electrodes modified with Y-shaped peptides exhibited excellent antifouling and electrochemical sensing performances. The developed biosensor was able to effectively resist biofouling in various protein solutions and even serum samples, and the linear range of the biosensor for human IgG detection was from 100 pg mL^{-1} to 10 μg mL^{-1}, with a relatively low limit of detection of 32 pg mL^{-1} (S/N = 3). The antifouling biosensor possesses the capability of assaying human IgG in real serum samples, and this strategy of developing low fouling biosensors based on Y-shaped peptides can be readily expanded to the construction of other biosensing systems for different targets.

1. Introduction

Early diagnosis and treatment are critical to the successful cure of diseases (e.g., cancer), which can effectively reduce treatment trauma, human suffering and even mortality (Dai et al., 2020; Jiang et al., 2020; Wu et al., 2015). Since the pathogenic process of diseases is often accompanied by the noticeable changes of some special biomolecules (known as disease markers), it is of great significance to achieve the sensitive detection of disease markers. Over the past few decades, qualitative leaps have been realized in fields of disease markers detection. Promising approaches for disease markers detection have been developed, including enzyme-linked immunosorbent assay (ELISA) (Alberti et al., 2014), surface plasmon resonance (SPR) (Law et al., 2011), fluorescence (Mizusawa et al., 2012; Rana et al., 2012) and electrochemical analysis (Chikkaveeraiah et al., 2012; Labib et al., 2013), and other technologies. Among them, electrochemical assay provides an excellent and popular choice for disease markers detection because of its advantages such as high sensitivity, low-cost, and user-friendly control (Mani et al., 2012; Radhakrishnan et al., 2013; Wang et al., 2015). Nevertheless, electrochemical signals are easy to be interfered by nonspecific adsorption of proteins or other organisms on their sensing interfaces, which are high sensitivity to tiny changes. This shortcoming hinders clinical application of electrochemical sensing systems in complex biological substrates (e.g., fetal bovine serum (FBS), human serum, and human blood samples). Therefore, surface fouling related to nonspecific adsorption remains a challenging issue that needs to be addressed for electrochemical biosensors.

From this perspective, antifouling materials are very important for the fabrication of low fouling biosensors. Although polyethylene glycol (PEG) (Cui et al., 2016; Hui et al., 2017; Wang et al., 2017) and oligo (ethylene glycol) (OEG) (Islam et al., 2014, 2019bib_Islam_et_al_2014bib_Islam_et_al_2019) are still extensively used in the construction of antifouling layers, and they do perform very well in preventing non-specific protein adsorption, some disadvantages (e.g., poor water-solubility, easily oxidative damage) have been reported in many literatures, which limited its further application (Liu et al., 2019;

* Corresponding author.
E-mail addresses: xiliangluo@qust.edu.cn, xiliangluo@hotmail.com (X. Luo).

https://doi.org/10.1016/j.bios.2021.113016
Received 14 December 2020; Received in revised form 10 January 2021; Accepted 15 January 2021
Available online 21 January 2021

Song et al., 2020). Therefore, peptides have recently been applied as potential antifouling materials with excellent biocompatibility, easily synthesized and stored, cost-effective, and tunable structures (Beyer et al., 2020; Zhang et al., 2013). More and more antifouling peptide sequences have been reported. For instance, the sequence (EKEKEKEPPPPC) designed by Jiang's group (Nowinski et al., 2012), and the sequences of (CPPPPNQNQNQNQDHWRGWVA) (Liu et al., 2018), (CPPPPEK2 (EK)4 (EK)) (Liu et al., 2019), and (CAEAEPPPPQEQKQEQK) (Han et al., 2020) reported by our group. According to previous reports (White et al., 2012; Yuan et al., 2020), lysine (K) and glutamic acid (E) occupied the surface of many peptides or proteins, and the sequence of alternating E and K, in aspect of alleviating protein adsorption, was better than other peptide sequences synthesized from natural amino acids. Meanwhile, some peptide fragments were also selected as recognizing receptors, which can be easily connected to other antifouling peptides. For example, aminopeptidase N (APN) can be identified by the (YVEYHLC) fragment (Song et al., 2020; Wang et al., 2014), the peptide sequence (HSSKLQK) can be recognized and cut by prostate-specific antigen (PSA) (Ding et al., 2019; Hun et al., 2015), and the peptide sequence (HWRGWVA) can recognize and detect IgG (Liu et al., 2018; Zhang et al., 2013).

Based on these excellent properties of various peptides, in this work, a newly Y-shaped peptide (CPPPPEK (HWRGWVA)EKEKE) with both recognizing and antifouling branches was designed, and then attached to electrode surface via the gold-sulfur bond to construct an antifouling biosensor (Scheme 1). This Y-shaped peptide contains two branches: one branch with a sequence of (EKEKEKE) for antifouling, and the other one with a sequence of (HWEGWVA) for recognizing a typical protein IgG. The electrode was firstly modified with conducting polymer poly (3,4-ethylenedioxythiophene) (PEDOT) doped with citrate through electrochemical polymerization, and gold nanoparticles (AuNPs) were then electrodeposited on modified electrode surface. The PEDOT-citrate can help to increase the effective electrode surface area for electron transfer, while AuNPs can be benefit to form Au–S bond for peptide immobilization. The Y-shaped peptide-based antifouling sensing system was thus successfully constructed and employed in the detection of human IgG in complex biological fluids.

2. Materials and methods

2.1. Reagents

Y-shaped peptide with the sequence of CPPPPEK(HWRGWVA) EKEKE (purity > 95%) and straight peptide with the sequence of CPPPPEKEKEKEHWRGWVA (purity > 95%) were designed by our group, and synthesized and purified by Hefei Bank-peptide Biotechnology Co., Ltd. (Hefei, China). The chromatogram chart and MS spectrum of the branched peptide are displayed in the Supporting Information (Figure S1). Human immunoglobulin G (IgG, purity > 95%), myoglobin (Mb), and lysozyme (Lys) were bought from Beijing Solarbio Science & Technology Co., Ltd. (Beijing, China). Sodium citrate and 3,4-ethylenedioxythiophene (EDOT) were obtained from Tianjin Bodi Chemical Industry Co., Ltd. (Tianjin, China) and Aladdin Regents (Shanghai, China), respectively. Albumin bovine fraction V (BSA, purity > 98%) was offered by Xinke Zhongjing Biological Technology Co., Ltd. (Beijing, China). FITC labelled BSA, carcino-embryonic antigen (CEA), human serum albumin (HSA), and α-fetoprotein (AFP) were ordered from Adamas Reagent, Ltd. (Shanghai, China). CA15-3 was obtained from Abcam (Cambridge, UK). The used human serum and blood samples were from the Qingdao 8th People's Hospital (Qingdao, China), and all samples were used with the consent and understanding of the patients. All the clinic samples were prepared and used under the relevant institution and law permits, and the authorization of the organizational review committee of Qingdao 8th People's Hospital (Qingdao, China) was obtained. The deionized water was prepared from Milli-Q water clarification equipment (18 MΩ/cm). Other reagents used were all of the analytical grade.

2.2. Instruments

Scanning electron microscopy (SEM) images were monitored by the Regulus 8100 instrument (Hitachi Company, Japan). ESCALAB 250Xi spectrometer (Thermo VG Fisher Scientific, USA) was applied for the characterization of X ray photo-electron spectrometry (XPS), which contains a monochromatic Al Kα X-ray source ($h\nu$ = 15 kV), via normalizing the C (1s) peak (284.6 eV) to calibrate all spectra. Surface hydrophilic properties of various constructed interfaces were characterized by measuring the water contact angle (WCA) with the JC 2000D1 Instrument (Shanghai Zhongchen Digital Equipment Company, China). Confocal laser microscope TCS-SP5 instrument (Leica, Germany) was used to check the image of fluorescein-labelled protein adsorption. Zeta potential (ζ) of the Y-shaped peptide was measured by the Zetasizer Nano-ZS (Malvern Instruments, USA). Circular dichroism (CD) data of the Y-shaped peptide was carried out with a Jasco J-1100 CD Spectrophotometer (Jasco Incorporated, Japan).

Cyclic voltammetry (CV), differential pulse voltammetry (DPV), and

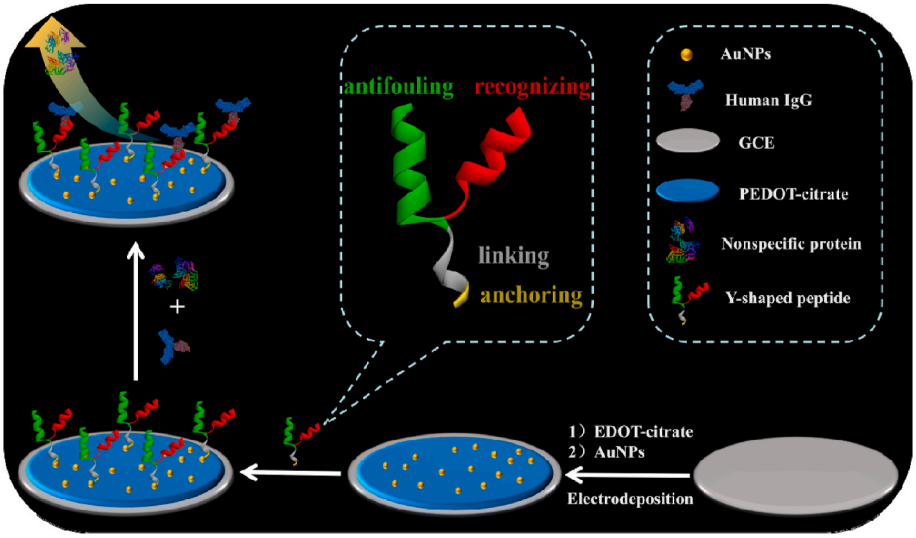

Scheme 1. Schematic diagram for the fabrication of antifouling biosensor based on designed Y-shaped peptides.

electrodeposition experiment were performed by the electrochemical workstation CHI 660E/CHI 760D (Shanghai CH Instruments Company, China), with a three-electrode test system (Pt wire as the counter electrode, saturated calomel CHI150 as the auxiliary electrode, bare or modified glassy carbon electrode (GCE, diameter 3.0 mm) as the working electrode). All experimental operations, except where noted, were implemented at room temperature. Under the amplitude of 50 mV, DPV tests were performed at the range of −0.2 to 0.6 V, with the scan rate, initial and final potential set at 0.1 V s^{-1}, −0.2 V and 0.6 V, respectively. All the electrochemical measurements were carried out in the phosphate buffered saline (PBS, pH 7.4, 0.01 M) with 5.0 mM $[Fe(CN)_6]^{3-/4-}$ and 100 mM KCl.

2.3. Characterization of the Y-shaped peptide

Zeta potential (ζ) of the Y-shaped peptide was recorded with the concentration of 1.0 mg mL^{-1}. CD spectra in a wavelength range of 190–270 nm was tested to prove the secondary structure of Y-shaped peptides (the concentration of the Y-shaped peptide was 0.2 mg mL^{-1}). Isoelectric point (pI) of the Y-shaped peptide was calculated theoretically.

2.4. Preparation of the antifouling biosensor

Before modification, the bare GCE were polished by 1.0, 0.3, and 0.05 μm micro-polish powder, respectively, and then ultrasonically rinsed sequentially using water, absolute ethanol, and water for 3 min each time. The modification of PEDOT-citrate was performed according to previous report with slight modification (Song et al., 2020). Briefly, 5.0 mL mixed solution composed of 0.02 M EDOT and 43.4 mg sodium citrate were prepared, and the electrochemical deposition was carried out at a constant potential of 1.1 V (vs SCE) for 200 s. Afterword, AuNPs were electrodeposited on the GCE/PEDOT-citrate surface by CV method with 4 sweep segments between −1.5 and 0.5 V (Han et al., 2020), in 4.0 mL solution containing 0.5 mM chloroauric acid ($HAuCl_4$) and 0.5 M KNO_3. Finally, the PEDOT-citrate/AuNPs modified electrode was incubated in 0.2 mg mL^{-1} Y-shaped peptide solution for 12 h, to immobilize the Y-shaped peptide on the AuNPs through the connection of Au–S bonds. The antifouling biosensor was thus fabricated, and it was stored at 4 °C for further use.

2.5. Interface antifouling assessment

Solutions of pure proteins with different charges, and complex biological samples (human serum and blood samples) were selected to assess the antifouling performances of different modified electrodes. The DPV current signals of various electrodes before (I_0) and after (I) soaking in protein solutions or complex samples for 30 min was measured to indicate the antifouling effect. Before tested in human sera and blood samples, the biosensor interfaces were first saturated with 1.0 mg mL^{-1} IgG solution, so as to exclude the effect of specific target IgG binding in these biological samples. Biological samples used in the tests were diluted with PBS to various concentration (V/V). Meanwhile, fluorescence images of three modified interfaces after incubation in 0.2 mg mL^{-1} FITC fluorescent labelled BSA protein for 30 min were examined by using the Leica TCS-SP5 microscope.

2.6. Sensing of the human IgG

The prepared biosensor was soaked in IgG solutions with various concentration for 90 min at room temperature, and the DPV peak current changes before and after the specific binding of IgG were recorded as the sensing signal.

2.7. Clinical patient sample preparation

Clinical human serum was obtained from the patient blood after centrifugation for 5 min at 10,000 r·min^{-1}. Then the supernatant (i.e., clinical human serum samples) was frozen at −80 °C for later use. Before detection with the biosensor, the frozen serum was taken out and diluted with 0.01 M PBS solution.

3. Results and discussions

3.1. Investigation of the Y-shaped peptides

To avoid non-specific adsorption of proteins, in general, we should choose the peptides with excellent hydrophilic property and neutral in overall charge. Previous reports about peptides for antifouling purpose were all basically based on linear peptides, and biosensors based on branched peptides were rarely reported, especially those based on multifunctional branched peptides. Herein, a new Y-shaped branched peptide was designed, and the chemical formula of the Y-shaped peptide was shown in Figure S2. Theoretical calculation revealed that the isoelectric point (pI) of this branched peptide is 7.05, and the measured zeta potential (ζ) is +2.259 mV (Fig. 1A), which is slightly positively charged but close to neutral. In order to illustrate the secondary structure of the Y-shaped peptides, the CD spectrum was tested (Fig. 1B). The results of a high peak (−) near 200 nm and a lower peak (+) at 226 nm indicated a helix structure of the amino acid proline (P), and further indicated a high graft density of the peptides (Nowinski et al., 2012).

3.2. Characterization of the biosensor fabrication process

The fabrication strategy of this Y-shaped peptide based sensing system was shown in Scheme 1. To evaluate the feasibility of the experiment, each fabrication process was recorded by DPV measurement (Fig. 1C). Clearly, the bare GCE had a relatively high current value, in contrast to that of the GCE/PEDOT-citrate. This was due to the charge repulsive interaction between the PEDOT-citrate surface with negative charge and the negative $[Fe(CN)_6]^{3-/4-}$ molecules. After the electrochemical deposition of AuNPs, a rise of the current signal was observed, owing to the excellent electrical conductivity of AuNPs. When the modified electrode was further combined with the Y-shaped peptides and the special IgG targets successively, the current signals continued to decrease accordingly, owning to the fact that the immobilized peptides and the captured IgG hampered the electron transfer of the redox molecules to the electrode surface. These monitored changes in each step indicated successful fabrication of the biosensor, and the current changes associated with the IgG binding offered signals for target detection.

The morphology features of various modified electrode surfaces were characterized by SEM. Sodium citrate doped PEDOT film presented a uniform but coarsely grained surface. After the electrodeposition of gold nanoparticles, a layer of uniformly distributed gold nanoparticles can be seen on the modified electrode surface, as shown in Fig. 1D.

The hydrophilic property of various electrode surfaces was tested by the water contact angle (Figure S3 and Table S1). The contact angles of the surfaces of the bare GCE, GCE/PEDOT-citrate, GCE/PEDOT-citrate/AuNPs, and GCE/PEDOT-citrate/AuNPs/Y-shaped peptide were (62.4 ± 0.2)°, (42.7 ± 0.2)°, (48.0 ± 0.2)°, (30.1 ± 0.2)°, respectively. This can be obviously observed that the contact angle was greatly reduced after the immobilization of the Y-shaped peptides, because of the strong hydrophilicity of the Y-shaped peptides, which is beneficial for antifouling performance.

To further prove the successful construction of the biosensor, XPS was chosen as a persuasive characterization. As can be seen in Fig. 1E, the sodium citrate doped PEDOT modified electrode surface mostly contains three elements: oxygen (O), carbon (C) and sulfur (S). After the electrodeposition of AuNPs, the peak of the element gold (Au) can be

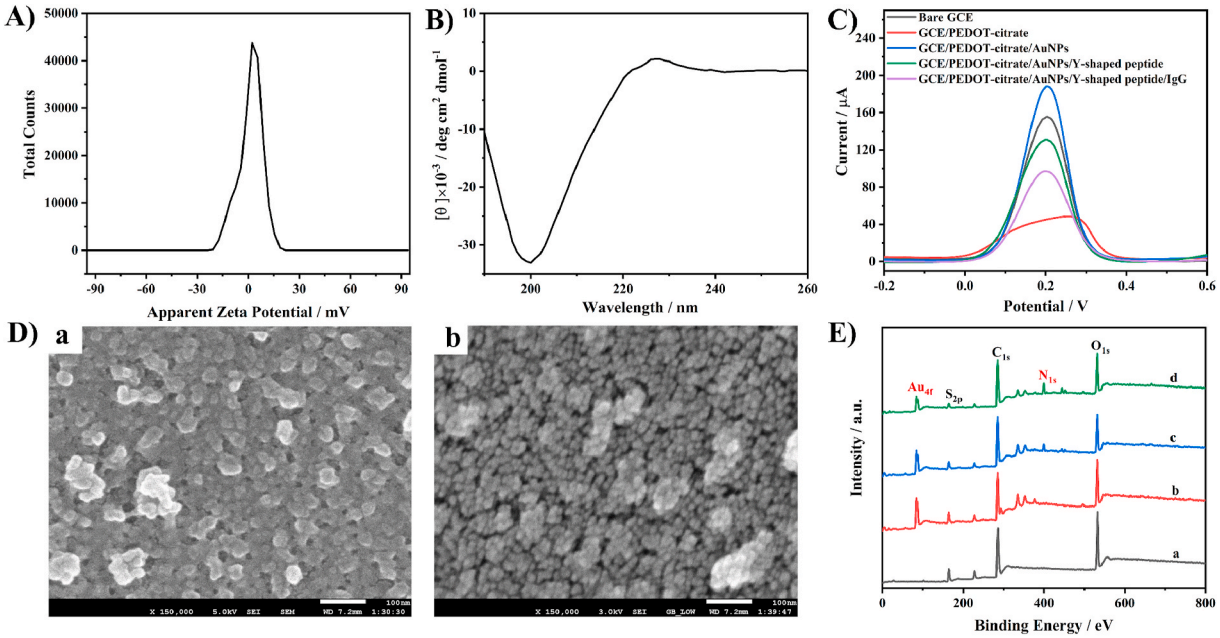

Fig. 1. (A) Zeta potential of the designed Y-shaped peptide. (B) CD spectra of 0.2 mg mL^{-1} designed Y-shaped peptide in PBS. (C) DPV responses of different electrodes in 5.0 mM $[Fe(CN)_6]^{3-/4-}$ solution. (D) SEM images of electrode surfaces modified with the PEDOT-citrate (a) and the PEDOT-citrate/AuNPs (b). (E) XPS graphics of the PEDOT-citrate (a), PEDOT-citrate/AuNPs (b), PEDOT-citrate/AuNPs/Y-shaped peptide (c), and PEDOT-citrate/AuNPs/Y-shaped peptide/IgG (d) modified electrodes.

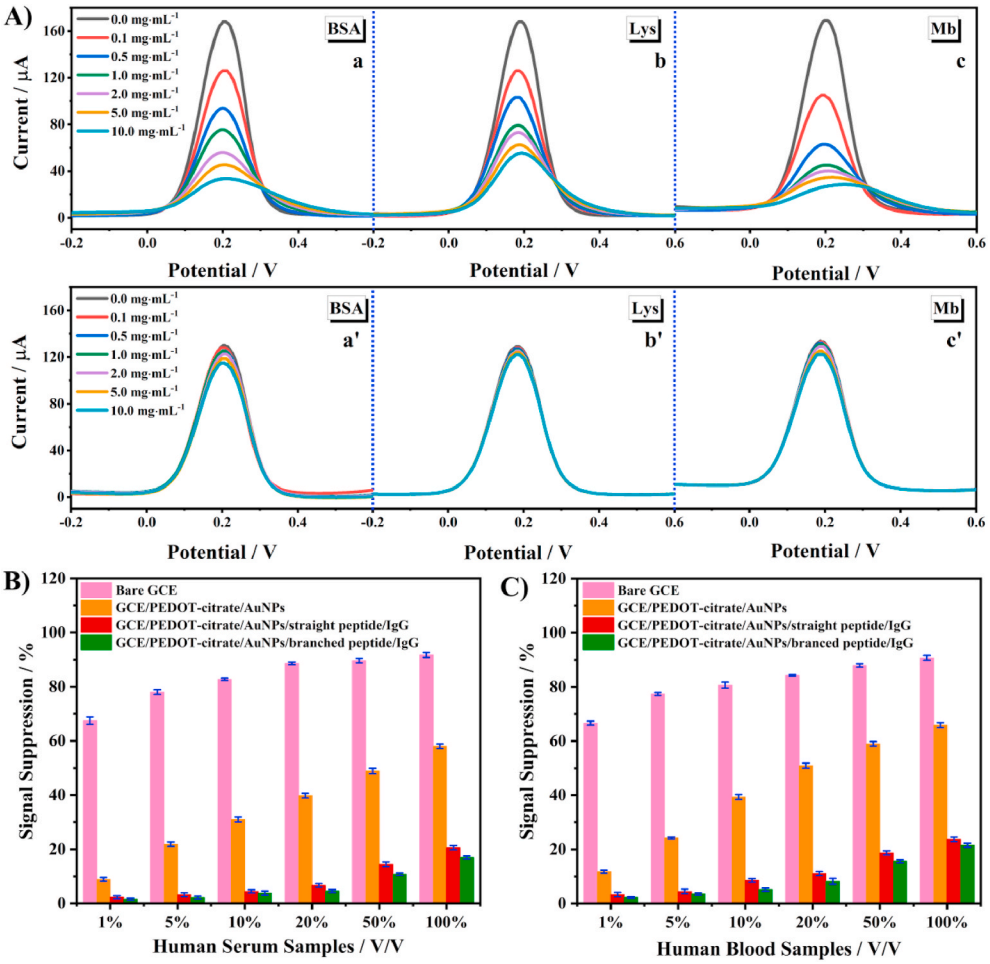

Fig. 2. (A) DPV response curves of the bare GCE (a, b, c) and the GCE/PEDOT-citrate/AuNPs/Y-shaped peptide (a', b', c') after soaking in various concentrations of BSA (a-a'), Lys (b-b'), and Mb solutions (c-c'), respectively. The DPV measurements were carried out in 5.0 mM $[Fe(CN)_6]^{3-/4-}$ solution. The antifouling properties comparison of four interfaces (bare GCE, GCE/PEDOT-citrate/AuNPs, GCE/PEDOT-citrate/AuNPs/straight peptide/IgG, and GCE/PEDOT-citrate/AuNPs/Y-shaped peptide/IgG) in different concentration of (B) human serum samples (V/V) and (C) blood samples (V/V).

clearly observed. As peptides are rich in nitrogen (N) element, when the peptides are attached successfully to the modified electrode surface, the peak of N element was observed. Human IgG, as a target, is also rich in N element. Consequently, after IgG conjugation, XPS spectrum shows significant increase in the peak of N element. These XPS characterizations revealed effective immobilization of the peptides and the following binding of target IgG, and the successful construction of the biosensor step by step.

3.3. Antifouling performances

Herein, the antifouling property of the designed Y-shaped peptide modified electrode was evaluated by DPV detection. The peptide based biosensors were immersed in different protein solutions for 30 min with BSA (negatively charged), Lys (positively charged), and Mb (neutral in charge), respectively. And DPV response curves of the biosensors in these three kinds of protein solutions were summarized in Fig. 2A. As expected, slight current changes of the biosensors were observed after soaking in various concentrations of protein solutions (a', b', c' of Fig. 2A), indicating acceptable antifouling performances of the biosensors in these protein solutions. In contrast, very significant current changes of the bare electrodes were observed after soaking in similar protein solutions (a, b, c of Fig. 2A). These results clearly exhibited that the Y-shaped peptides modified electrode surfaces were capable of effectively resisting nonspecific protein adsorption.

Based on these encouraging results, the antifouling performance of the Y-shaped peptide based biosensor was then tested in complex biological liquids (human serum and blood samples). As demonstrated in Fig. 2B and C, the signal suppression rate of the biosensor (GCE/PEDOT-citrate/AuNPs/Y-shaped peptide) was less than 5% after soaking in 20% patient serum, or in 10% human blood samples (compared with human whole blood samples, there were no fibrinogen and coagulation factor in human serum, which may be the reason for such difference). These results further proved excellent antifouling capability of the Y-shaped peptide modified interface, and the possibility of this biosensor for target detection in real serum samples. Although the antifouling performance of the biosensor based on Y-shaped peptide was superior to that based on the straight peptide, its antifouling performance still needs to be further improved in complex biological media such as 100% serum. Besides, more intuitive characterization was performed with laser confocal imaging, as shown in Fig. 3. Compared with the bare and the PEDOT-citrate/AuNPs modified surfaces, where clear fluorescent intensity indicating severe nonspecific protein (FITC labelled BSA) adsorption were observed. The Y-shaped peptide modified surface exhibited excellent antifouling ability, and no obvious fluorescence was observed after similar treatment with FITC labelled BSA.

Meanwhile, the variation of the antifouling ability of the Y-shaped peptide based biosensor along with the extension of time was also investigated in 20% human serum (Figure S4). It is clear that the antifouling abilities of all the electrode surfaces decreased (signal suppression increased) along with the extension of the time, but the Y-shaped peptides modified surface exhibited a variation much less than that of other electrode surfaces. Moreover, comparing the antifouling abilities of the designed Y-shaped peptide and the control peptide (straight peptide), we found that the Y-shaped peptide outperformed the straight peptide in the aspect of antifouling performance. This should be ascribed to the water permeability and steric repulsion (Liu et al., 2017, 2019bib_Liu_et_al_2017bib_Liu_et_al_2019), and previous reports have indicated that the presence of the intramolecular and intermolecular cavities promoted the water transportation. (Choudhury et al., 2018; Suriyanarayanan et al., 2013; Selim et al., 2017).

3.4. Detection of the human IgG

Under the optimized experimental conditions (0.2 mg mL^{-1} Y-shaped peptide and 90 min hybridization time, Figure S5), the sensing performance of the Y-shaped peptide based biosensor towards various concentrations of human IgG was investigated by DPV. As exhibited in Fig. 4A, the DPV current signal decreased with the increasing of the content of human IgG. This phenomenon was caused by the binding and accumulation of IgG on the sensing interface which leads to the obstruction of the electron transfer. The current changes (I_0–I) before and after incubation with human IgG is linearly related to the concentration of IgG in the range of 0.1–10000 ng mL^{-1} (R^2 = 0.9954)

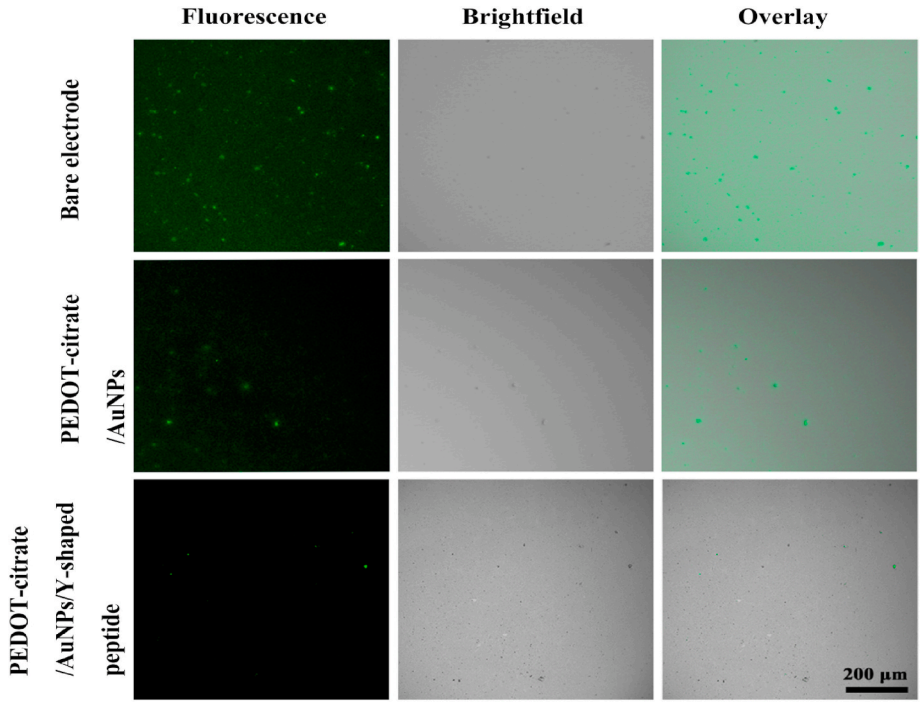

Fig. 3. Laser confocal imaging of the bare electrode (first line), PEDOT-citrate/AuNPs (second line), and PEDOT-citrate/AuNPs/Y-shaped peptide (third line) modified electrodes after soaking in 0.2 mg·mL^{-1} FITC labelled BSA for 30 min.

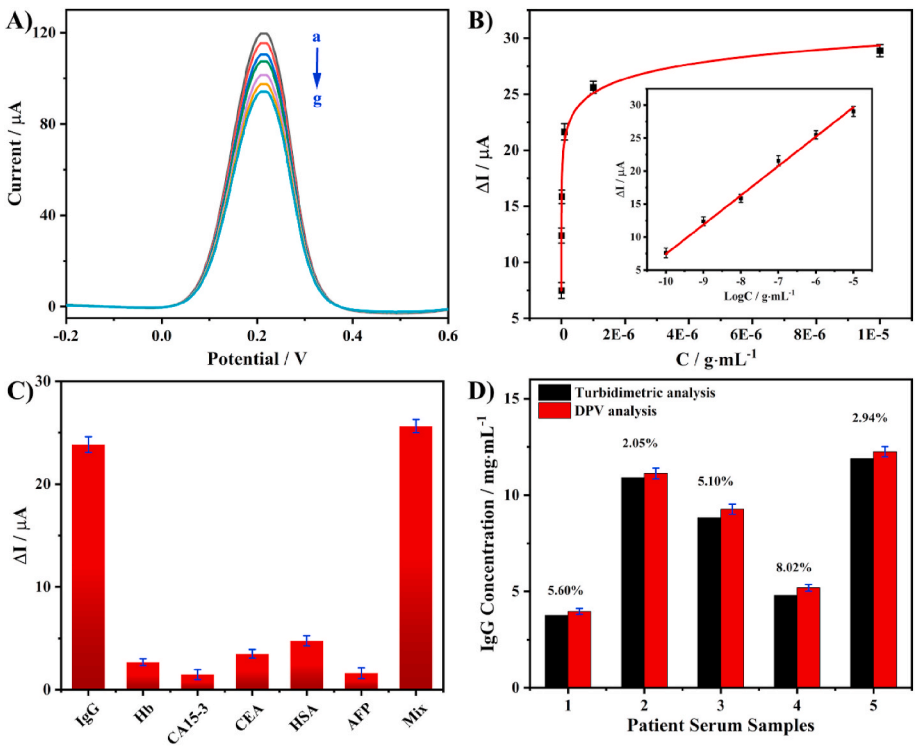

Fig. 4. (A) DPV response curves of the Y-shaped peptide-based biosensor to human IgG. Curves a to g refers to 0, 0.1, 1, 10, 100, 1000, 10,000 ng mL^{-1} human IgG, respectively. (B) Current difference ($\Delta I = I_0 - I$) after incubation with various contents of human IgG in 5.0 mM $[Fe(CN)_6]^{3-/4-}$ probe. Inset shows the corresponding calibration curve (R^2 = 0.9954). (C) Current changes (I_0–I) of the human IgG biosensor to IgG (1.0 μg mL^{-1}), and Hb (1.0 mg mL^{-1}), CA15-3 (1.0 mg mL^{-1}), CEA (1.0 mg mL^{-1}), HSA (1.0 mg mL^{-1}), AFP (1.0 mg mL^{-1}), and their mixture (Mix), respectively. (D) Comparative analysis results of clinic patient serum samples measured by hospital turbidimetric method (black) and the biosensor (red). (For interpretation of the references to colour in this figure legend, the reader is referred to the Web version of this article.)

(Fig. 4B). This limit of detection (LOD) was estimated to be 0.032 ng mL^{-1} (S/N = 3). Compared with previous reported results (Table S2), this Y-shaped peptide based biosensor exhibited better linear range and lower LOD, indicating the advantages of using the designed Y-shaped peptides for biosensor construction.

3.5. Selectivity, stability and reproducibility of the biosensor

In order to investigate the selectivity of the Y-shaped peptide based biosensors, 1.0 μg mL^{-1} human IgG, and 1.0 mg mL^{-1} Hb, CA15-3, CEA, HSA, AFP, and their mixed solution were detected with the biosensor, respectively. As shown in Fig. 4C, the biosensor showed good selectivity toward target IgG, and even in the existence of much higher concentrations of various interferences (1000 times), the biosensor still remained almost unaffected.

For the stability investigation of the biosensor, the continuous CV scan (Figure S6A) was tested with the constructed biosensor (GCE/PEDOT-citrate/AuNPs/Y-shaped peptide). The results indicated that the current value remained fairly consistent after 100 sweep segments. Furthermore, the prepared Y-shaped peptide based biosensors were stored in PBS for 12 days at 4 °C, and the signal retention rate approximately achieved 97% (Figure S6B), indicating excellent stability of the Y-shaped peptide based biosensor.

The reproducibility of the Y-shaped peptide based biosensor was measured by detecting 1.0 μg mL^{-1} target IgG with 7 different modified electrodes (Figure S6C), and the relative standard deviation (RSD) was 2.66%. The signal changes of the same modified electrode after hybridization with 1.0 μg mL^{-1} target IgG were measured by continuous scanning for 7 times (curve a of Figure S6D), and the RSD was 0.58%. The biosensor was stored in PBS (pH 7.4, 0.01 M) at 4 °C, and then its DPV responses were measured for 7 times with intervals of 30 min (curve b of Figure S6D), and the RSD was measured to be 2.62%. These results proved excellent reproducibility of the prepared biosensor.

In this study, the regeneration of the constructed biosensor was evaluated by soaking the Y-shaped peptide modified electrode into a regeneration solution containing 0.6% ethanol and 6.0 mM NaOH. After detecting target IgG, the biosensor was soaked in the regeneration solution for 10 min to release associated IgG, and then thoroughly rinsed with PBS buffer before the next DPV detection. As illustrated in Figure S7, the biosensor can be reused for at least 5 times without significant change or decrease in its response.

3.6. Sample analysis of clinical serum

Immunoturbidimetry is a commonly used method for IgG detection in most hospitals. To demonstrate the potential of the developed biosensors for clinic application, the biosensors were used for the determination of different real patient serum samples, and then the assaying results were compared with those measured with the immunoturbidimetry method in the hospital. Interestingly, the IgG concentrations of clinical serum samples measured with the development biosensors were basically consistent with those assayed by the hospital method, as shown in Fig. 4D, indicating that the developed biosensor based on the Y-shaped peptides possesses an acceptable accuracy in assaying of clinical serum samples.

4. Conclusions

To summarize, an ultralow fouling electrochemical biosensor for the detection of human IgG was developed based on the designed Y-shaped peptide with both recognizing and antifouling branches. The electrochemical biosensor has revealed excellent performance with high specificity, selectivity, sensitivity (with the limit of detection of 32 pg mL^{-1}), and stability. More importantly, thanks to the unique design of the Y-shaped branched peptide, the fabrication process of this antifouling biosensor was considerably simple, and the antifouling performance the biosensor based on the Y-shaped peptide was superior to that based on the straight peptide in complex biological media including serum. The antifouling biosensor was capable of assaying IgG in serum samples with satisfying accuracy, demonstrating its great potential for practical clinical applications. In addition, the strategy of constructing antifouling biosensors simply based on designed Y-shaped peptides reported in this work can be easily extended to the development of other antifouling sensing systems.

CRediT authorship contribution statement

Min Chen: Conceptualization, Methodology, Investigation, Writing - original draft, Visualization, Data curation. **Zhen Song:** Conceptualization, Data curation, Writing - review & editing. **Rui Han:** Resources, Data curation, Writing - review & editing. **Yang Li:** Writing - review & editing. **Xiliang Luo:** Conceptualization, Methodology, Investigation, Writing - review & editing, Visualization, Supervision, Funding acquisition.

Declaration of competing interest

The authors declare that they have no known competing financial interests or personal relationships that could have appeared to influence the work reported in this paper.

Acknowledgment

This work is supported by the National Natural Science Foundation of China (21974075, 21675093), and the Taishan Scholar Program of Shandong Province of China (ts20110829).

Appendix A. Supplementary data

Supplementary data to this article can be found online at https://doi.org/10.1016/j.bios.2021.113016.

References

Alberti, D., van't Erve, M., Stefania, R., Ruggiero, M.R., Tapparo, M., Geninatti Crich, S., Aime, S., 2014. Angew. Chem. Int. Ed. 53 (13), 3488–3491.
Beyer, C.D., Reback, M.L., Heinen, N., Thavalingam, S., Rosenhahn, A., Metzler-Nolte, N., 2020. Langmuir 36 (37), 10996–11004.
Chikkaveeraiah, B.V., Bhirde, A.A., Morgan, N.Y., Eden, H.S., Chen, X., 2012. ACS Nano 6 (8), 6546–6561.
Choudhury, R.R., Gohil, J.M., Mohanty, S., Nayak, S.K., 2018. J. Mater. Chem. 6 (2), 313–333.
Cui, M., Song, Z., Wu, Y., Guo, B., Fan, X., Luo, X., 2016. Biosens. Bioelectron. 79, 736–741.
Dai, X., Hao, J.-N., Gu, J., Li, Y., 2020. ACS Appl. Bio Mater. 3 (6), 3792–3799.
Ding, C., Wang, X., Luo, X., 2019. Anal. Chem. 91 (24), 15846–15852.
Han, R., Wang, G., Xu, Z., Zhang, L., Li, Q., Han, Y., Luo, X., 2020. Biosens. Bioelectron. 164, 112317.
Hui, N., Sun, X., Niu, S., Luo, X., 2017. ACS Appl. Mater. Interfaces 9 (3), 2914–2923.
Hun, X., Xu, Y., Luo, X., 2015. Microchim. Acta 182 (9–10), 1669–1675.
Islam, N., Gurgel, P.V., Rojas, O.J., Carbonell, R.G., 2014. J. Phys. Chem. C 118 (10), 5361–5373.
Islam, N., Gurgel, P.V., Rojas, O.J., Carbonell, R.G., 2019. Bioconjugate Chem. 30 (3), 815–825.
Jiang, C., Wang, G., Hein, R., Liu, N., Luo, X., Davis, J.J., 2020. Chem. Rev. 120 (8), 3852–3889.
Labib, M., Khan, N., Ghobadloo, S.M., Cheng, J., Pezacki, J.P., Berezovski, M.V., 2013. J. Am. Chem. Soc. 135 (8), 3027–3038.
Law, W.-C., Yong, K.-T., Baev, A., Prasad, P.N., 2011. ACS Nano 5 (6), 4858–4864.
Liu, N., Hui, N., Davis, J.J., Luo, X., 2018. ACS Sens. 3 (6), 1210–1216.
Liu, N., Song, J., Lu, Y., Davis, J.J., Gao, F., Luo, X., 2019. Anal. Chem. 91 (13), 8334–8340.
Liu, Z., An, X., Dong, C., Zheng, S., Mi, B., Hu, Y., 2017. J. Mater. Chem. 5 (44), 23190–23197.
Mani, V., Periasamy, A.P., Chen, S.-M., 2012. Electrochem. Commun. 17, 75–78.
Mizusawa, K., Takaoka, Y., Hamachi, I., 2012. J. Am. Chem. Soc. 134 (32), 13386–13395.
Nowinski, A.K., Sun, F., White, A.D., Keefe, A.J., Jiang, S., 2012. J. Am. Chem. Soc. 134 (13), 6000–6005.
Radhakrishnan, S., Sumathi, C., Umar, A., Jae Kim, S., Wilson, J., Dharuman, V., 2013. Biosens. Bioelectron. 47, 133–140.
Rana, S., Singla, A.K., Bajaj, A., Elci, S.G., Miranda, O.R., Mout, R., Yan, B., Jirik, F.R., Rotello, V.M., 2012. ACS Nano 6 (9), 8233–8240.
Selim, M.S., Shenashen, M.A., El-Safty, S.A., Higazy, S.A., Selim, M.M., Isago, H., Elmarakbi, A., 2017. Prog. Mater. Sci. 87, 1–32.
Song, Z., Chen, M., Ding, C., Luo, X., 2020. Anal. Chem. 92 (8), 5795–5802.
Suriyanarayanan, S., Lee, H.H., Liedberg, B., Aastrup, T., Nicholls, I.A., 2013. J. Colloid Interface Sci. 396, 307–315.
Wang, G., Xu, Q., Liu, L., Su, X., Lin, J., Xu, G., Luo, X., 2017. ACS Appl. Mater. Interfaces 9 (36), 31153–31160.
Wang, J., Xu, G., Wang, W., Xu, S., Luo, X., 2015. Chem. Asian J. 10 (9), 1892–1897.
Wang, W., Wei, Z., Zhang, D., Ma, H., Wang, Z., Bu, X., Li, M., Geng, L., Lausted, C., Hood, L., Fang, Q., Wang, H., Hu, Z., 2014. Anal. Chem. 86 (23), 11854–11859.
White, A.D., Nowinski, A.K., Huang, W., Keefe, A.J., Sun, F., Jiang, S., 2012. Chem. Sci. 3 (12).
Wu, L., Qu, X., 2015. Chem. Soc. Rev. 44 (10), 2963–2997.
Yuan, Z., Li, B., Niu, L., Tang, C., McMullen, P., Jain, P., He, Y., Jiang, S., 2020. Angew. Chem. Int. Ed. 59 (50), 22378–22381.
Zhang, Y., Islam, N., Carbonell, R.G., Rojas, O.J., 2013. ACS Appl. Mater. Interfaces 5 (16), 8030–8037.